

WiAnti: an Anti-interference Activity Recognition System based on WiFi CSI

Jinyang Huang^{*†}, Bin Liu^{*†}, Hongxin Jin^{*†}, Zhiqiang Liu^{*†}

^{*}School of Information Science and Technology, University of Science and Technology of China, Hefei, China

[†]Key Laboratory of Electromagnetic Space Information, Chinese Academy of Science, Hefei, China

huangjy@mail.ustc.edu.cn, flowice@ustc.edu.cn, {jhx0112,lzhq28}@mail.ustc.edu.cn

Abstract—As an important technology in the field of Internet of Things, activity recognition is a well-researched topic. Due to its characteristics of no-invasion, no privacy leakage, high recognition rate, and good user experience, Channel State Information (CSI)-based is a great approach to solve the activity recognition problem. However, commodity WiFi devices for identification are usually in a complex electromagnetic environment, where the interference caused by WiFi devices from channel overlap is the most severe. To solve the above problem, we propose WiAnti, a CSI-based activity recognition system which is robust to co-channel Interference. By adaptive subcarrier selection, WiAnti can achieve activity recognition with high accuracy. As demonstrated by experimental results, in the same scenario with co-channel interference, WiAnti yields 95.865% activity recognition accuracy rate on average, which improve the recognition rate by 8% on average over WiFall.

I. INTRODUCTION

Activity recognition systems have inspired novel user interfaces and new applications in smart cities, surveillance, emergency response, and military missions [1]. However, there are several problems in the development of the activity recognition, such as low recognition accuracy, privacy leaks and bad user experience [2]. To solve these problems, camera-based [3]–[5] and sensor-based [6], [7] recognition schemes have been well studied in the literature.

For the camera-based systems, such as KVMD [3], DSTIP [4] and Kinect [5], they are usually equipped with high-resolution cameras to record the body movement and classify these records into different activities. These camera-based activity recognition systems can obtain a high recognition accuracy. However, the environment condition has a great effect on the recognition accuracy, and the privacy problem limits the scope of its application. As for sensor-based recognition systems, multiple sensors attached to the body can monitor the motion information of different parts of the body, and then signal processing technology and classification technology [8], [9] are adopted to classify which kind of activities the current activity is [6], [7]. However, they need to perform the professional prior calibration by experts before normal work, in addition, the additional equipment worn on the body makes the user experience worse.

In recent years, with the rapid development in wireless techniques, several device-free approaches, such as Radio Frequency (RF)-based and WiFi-based, have attracted more and more attention due to the activity recognition without

wearing additional equipment on the body [10]–[14]. The RF-based recognition systems adopt the RF equipment to produce the RF waves, which are affected by the movement of human body [15], and the recognition accuracy of the RF-based systems is high. However, the specialized RF equipment is necessary. WiFi-based activity recognition systems can utilize the off-the-shelf WiFi devices without adopting other specialized equipment to monitor the activities in the Area of Interest (AoI). One sending WiFi device and one receiving WiFi device are placed in two different places of AoI, and the receiving WiFi device receives the regular signals from the sending WiFi device. The different activities have different effects on the receiving signals, therefore the effective signal processing methods can recognize different activities based on the receiving WiFi signals.

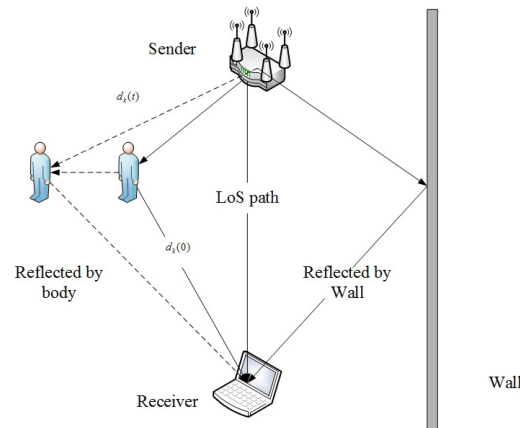


Fig. 1 Signal Propagation Model in Indoor Environment

WiFi-based activity recognition systems mainly utilize two different kinds of signals, the Received Signal Strength Indication (RSSI) [13], [14] and the Channel State Information (CSI) [10]–[12], to classify different activities. RSSI as the average measured power of a received radio signal [16] is a kind of coarse-grained radio channel measurement, and the performance of the RSSI-based systems is greatly affected by the link quality. In the complex environment, the multipath propagation will cause the fluctuations of the link quality, therefore the good performance cannot always be guaranteed [17]. Compared with RSSI, CSI is a fine-grained value derived

from the physical layer of the WiFi device, which can reflect the channel frequency response, to capture signal phase and amplitude information of different subcarriers. More information can be extracted to capture a subtle change of the link quality. Therefore, the CSI-based systems have the better robustness to the complex environment. As shown in Fig. 1, the link quality will change with the multipath due to the body movements, and the WiFi device can capture the changes and use them to recognize activities.

In the CSI-based activity recognition systems, the co-channel interference also has a great impact on the link quality, which will cause a bad performance due to the confusion between the activity and the co-channel interference. In the literature, no researcher has addressed this problem. To overcome the problem, we propose a CSI-based activity recognition system, **WiAnti**, which can effectively identify different activities in the scenario with the co-channel interference. The main contributions of this paper are expressed as three aspects:

- As far as we know, this work is the first to introduce the effect of co-channel interference on the CSI-based activity recognition system, and we propose a novel Anti-interference and Non-intrusive Activity Recognition System (WiAnti) leveraging CSI from a single commodity WiFi device.
- To analyze the effect of the co-channel interference, we carefully study the relationship between different subcarriers of CSI by experiment. The interference due to the overlap of WiFi channels will reduce the CSI packets per unit time, and the correlation between different subcarriers will be weakened.
- To improve the performance of WiAnti in the interference scenario, a subcarrier selection scheme is designed to dynamically choose several subcarriers with weak correlation, which can represent the changes caused by the interference. Then, the corresponding features are extracted and adopted to classify different activities with a high recognition accuracy.

The rest of the paper is organized as follows. Section II introduces related work. Section III presents background materials on CSI, CSMA/CA, IEEE 802.11n standard. Then, in Section IV, the impact of co-channel interference on CSI is shown and a CSI-based activity recognition system WiAnti is proposed. Next, the evaluation results through experiments are presented in Section V. Section VI concludes the paper.

II. RELATED WORK

Considering the characteristics of the no-invasion and awesome user experience, the device-free activity recognition approaches have attracted more and more attention [18]. According to the signal used for activity detection, existing device-free activity recognition systems can be grouped into three categories: RF-based, RSSI-based and CSI-based.

If a device-free activity recognition system ideally satisfies the following three features, it is possible to be deployed ubiquitously with existing infrastructure, which will easy to promote.

- **Informative measurements:** Contain information to recognize activity
- **Universal:** Use existing equipment or deployable on existing infrastructure
- **Robustness to Interference:** Reduce or eliminate the effects of interference

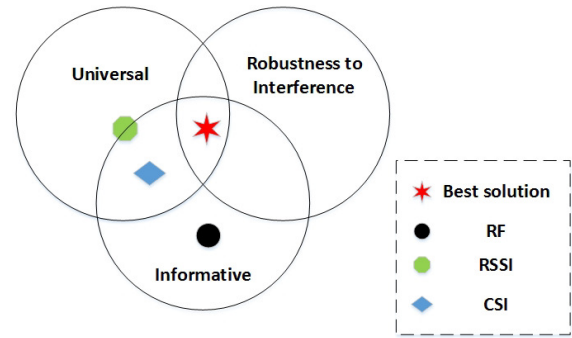


Fig. 2 Differentiating different approaches to device-free activity recognition

A Venn diagram with the three features of informative measurements, universal and robustness to interference is drawn. Fig. 2 is used to differentiate different approaches, and it shows which solution is capable of dealing with which requirements.

A. RF-based techniques

Fine-grained RF measurements can be obtained with using specialized hardwares, such as software defined radio (SDR) and universal software radio peripheral (USPR). The SDR can be adopted to measure the fluctuation of the strength of the received signal, which is caused by the movement of individuals. Then, the speed of human walking can be evaluated through the effective signal processing technology [19]. WiSee used USRP to capture the OFDM signals and measured the Doppler shift in signals reflected by bodies to recognize a set of nine different activities with a high accuracy [20]. However, all of these schemes need a specialized hardware to achieve a high activity recognition accuracy, which does not satisfy the universal requirement. The RF-based system can be expressed as a black circle in Fig. 2.

B. RSSI-based techniques

RSSI is an indication which measures the power of received radio signal. Because different activities cause different RSSI fluctuations, activities can be recognized with using the RSSI signals. PAWS designed an online activity recognition system, which explored WiFi ambient signals for RSSI fingerprint of different activities [13]. Wigest leveraged changes in WiFi signal strength to sense in-air hand gestures around the user's mobile device [13]. However, these approaches can only do coarse-grained activity recognition because RSSI falls entirely in the time domain, while frequency features are totally neglected. Suffering from performance degradation due to

multipath effect is also a problem for RSSI-based system [21]. The RSSI-based recognition system can be expressed as a green hexagon in Fig. 2.

C. CSI-based techniques

Compared with RSSI, CSI is a fine-grained value derived from the physical layer of the WiFi device. In CSI-based systems, features are descriptions of a motion from different perspectives, i.e., time domain and frequency domain. Frog Eye proposed a novel device-free crowd counting method based on CSI measurements [17]. E-eyes presented location-oriented activity identification such as cooking and gaming [10]. WiShop analyzed shopper's behavior through WiFi signals [22]. WiFall-1 exploited the special diversity of CSI to detect human fall in an indoor environment and used subcarrier fusion method for data dimension reduction [10]. Compared with WiFall-1, WiFall-2 used the subcarrier fusion method with frequency as a weight indicator [12]. However, most existing works do not consider the effects of co-channel interference, their experimental results are based on a non-disturbing environment, and the performance of these systems will degrade due to co-channel interference. The CSI-based system can be expressed as a blue diamond in Fig. 2. To overcome these drawbacks, we present WiAnti, a CSI-based activity recognition system which is robust to co-channel Interference. This means our proposed system WiAnti can deal with all the three requirements.

III. BACKGROUND

A. Overview of Channel State Information

In the frequency domain, the narrow-band flat-fading channel with multiple transmit and receive antennas (MIMO) can be modeled as:

$$\mathbf{y}_i = \mathbf{H}\mathbf{x}_i + \mathbf{n}_i \quad (1)$$

where i denotes the stream corresponding to the i^{th} transmit antenna and the receive antenna combination, \mathbf{x}_i , \mathbf{y}_i denote the transmitted and received signal vectors respectively, \mathbf{n}_i is the noise vector, \mathbf{H} is the channel matrix.

\mathbf{H} can be estimated at the receiver when a known sequence $\mathbf{x}_1, \mathbf{x}_2, \dots, \mathbf{x}_n$ is transmitted. As the IEEE 802.11n standard is a protocol based on OFDM technology, it divides the 2.4 to 2.4835 GHz band into 14 channels, each channel has 20M bandwidth and there are 56 subcarriers in each channel, so the estimated value of \mathbf{H} for N subcarriers can be represented as:

$$\mathbf{H} = [\mathbf{h}_1, \mathbf{h}_2, \dots, \mathbf{h}_j, \dots, \mathbf{h}_N]^T \quad (2)$$

In the above equation, the frequency response of k^{th} subcarrier can be expressed as:

$$\mathbf{h}_k = |\mathbf{h}_k| e^{j\sin \theta_k} \quad (3)$$

where $|\mathbf{h}_k|$ and θ_k are the amplitude and phase of the k^{th} subcarrier, respectively.

Using Intel 5300 Network Interface Card (NIC), WiAnti is capable of receiving six CSI streams simultaneously and 30 subcarriers in each stream. Therefore, 180 groups ($3 \times 2 \times 30$

of CSI values can be extracted from each packet, and the value of H can be represented as:

$$\mathbf{H}_{i,j} = \begin{bmatrix} h_{1,1} & h_{1,2} & h_{1,3} & \cdots & h_{1,30} \\ h_{2,1} & h_{2,2} & h_{2,3} & \cdots & h_{2,30} \\ \vdots & \vdots & \vdots & \ddots & \vdots \\ h_{6,1} & h_{6,2} & h_{6,3} & \cdots & h_{6,30} \end{bmatrix} \quad (4)$$

where $h_{i,k}$ is the CSI value for the k^{th} subcarrier in the i^{th} stream.

B. Carrier Sense Multiple Access with Collision Avoidance (CSMA/CA)

As a distributed protocol, CSMA is among the most widely implemented MAC protocols. In CSMA/CA, the backlogged node waits for a random period of silent time before transmitting, which is called back-off time. If no transmission is sensed by the node for the entire back-off time, the transmission of the node starts. Otherwise, the node defers as soon as it senses an ongoing transmission. When co-channel interference exists, the probability that the node senses an ongoing transmission becomes larger and the number of delays increases, which results in decreasing of the received packet number per unit time.

C. IEEE 802.11n standard for co-interference response

In CSMA/CA mechanism of IEEE 802.11n standard, a device can send packets only when it detects that all the sub-channels of the working channel are idle.

However, in the scenario with co-channel interference, the subcarriers of two channel overlaps in frequency spectrum, and the probability of packets being delayed for delivery increases. To deal with such problem, 802.11n standard uses a more flexible subcarrier power allocation method. The spectrally-overlapped subcarriers will be allocated more power, which lead to a greater advantage in competing for the sub-channels. On the contrary, because the subcarriers in non-overlapping areas have no need to compete, less power will be allocated to the subcarriers in non-overlapping areas. By this way, the ability for competing whole channel is improved. As a result, the correlations between subcarriers are weakened using the unbalanced power allocation method.

IV. SYSTEM DESIGN AND METHODOLOGY

In this section, the overall structure of WiAnti system is introduced.

A. System Overview

The workflow of the system WiAnti given in Fig. 3 contains four main parts: judgment of interference, adaptive data preprocessing, feature extraction and classification part.

The existence of the co-channel or adjacent-channel interference is judged in first part. Then, according to the judgment, different strategies can be adopted in the second part. In the scenario without co-channel interference, the data dimension will be reduced by subcarrier fusion. On the contrary, in the scenario with co-channel interference, the subcarrier selection

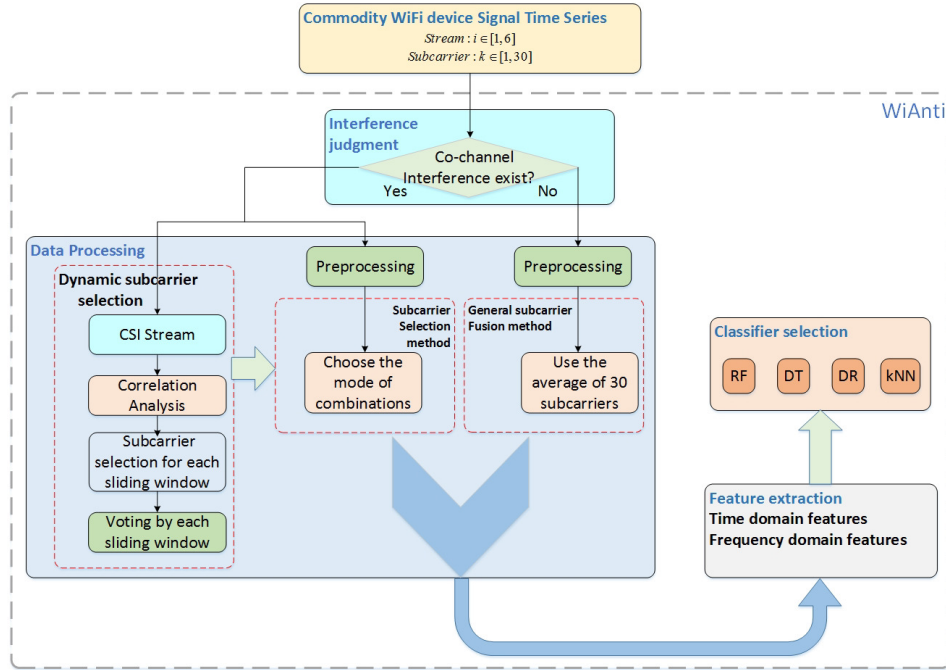


Fig. 3 WiAnti workflow

method will be used to improve the recognition accuracy rate. Next, the features will be extracted in the third part. Finally, the activities will be classified in the last part.

B. Co-channel Interference Detection

As introduced in Section III-B, in the scenario without co-channel interference, the channel is exclusive. The AP sends packets as usual and the number of received packets does not decrease per unit time. However, in the scenario with co-channel interference, the number of received packets per unit time decreases. Therefore, by recording the length of received packets per unit time, the existence of co-channel interference can be detected.

C. Correlation Judgment and Subcarrier Selection

In 802.11n standard, in order to compete for the channel, the power of spectrally-overlapped subcarriers increases, resulting in the corresponding subcarriers dominant in competing sub-channels. However, the subcarriers in non-interference area occupy sub-channels alone and do not need to compete, so the power of these subcarriers does not increase, which lead to the different power between the subcarriers in the spectrally-overlapped area and the non-overlapping area. However, the power difference causes the difference of each subcarrier's amplitude, and the correlations of subcarriers are weakened.

As shown in Fig. 4, the graph reflects the correlation matrix, each element in the matrix corresponds to the magnitude of the correlation coefficient between two subcarriers' amplitude. Red represents the correlation coefficient of 1 and blue represents the correlation coefficient of 0. Fig. 4(a)

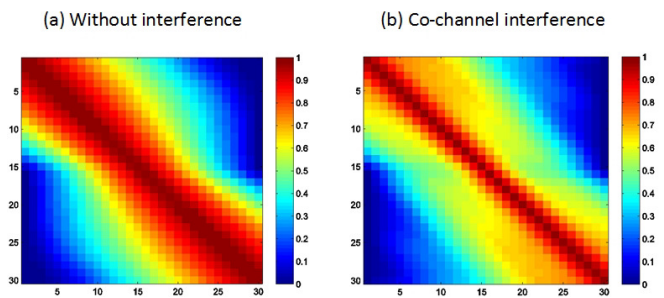


Fig. 4 Correlation Matrix of CSI Subcarriers in One Stream

depicts the strong correlation between 30 subcarriers in a stream without co-channel interference. When the number of spaced subcarriers between two subcarriers is less than 14, the correlation coefficient can reach more than 0.9. The correlation between the 30 subcarriers with co-channel interference is shown in Fig. 4(b). Compared to Fig. 4(a), the red covered area in Fig. 4(b) has a significantly thinner line, which represents the co-channel interference weakens the correlation between subcarriers.

However, since each action takes place in several seconds, the correlation matrix of a moment of CSI may not fully reflect the correlation between the subcarriers. For a fine-grained description of the correlation between subcarriers, the Pearson correlation coefficient of variation can be used to represent sequence correlation.

The Pearson correlation coefficient defines the strength of

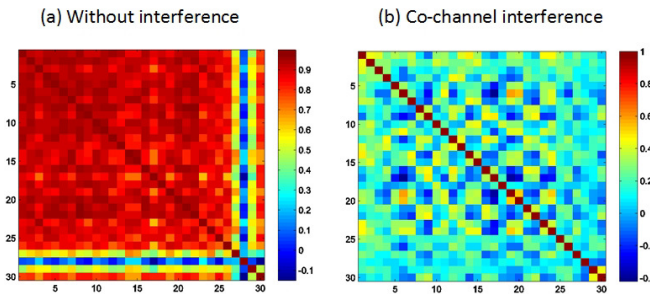


Fig. 5 Time series of each Subcarrier Correlation Matrix

the correlation using the covariance and standard deviation of the two variables (x and y):

$$r_{xy} = \frac{\sum_{t=1}^n (x_t - \bar{x})(y_t - \bar{y})}{\sqrt{\sum_{t=1}^n (x_t - \bar{x})^2} \sqrt{\sum_{t=1}^n (y_t - \bar{y})^2}} \quad (5)$$

where n is the length of sequence $x(n)$ and sequence $y(n)$. \bar{x} represents the mean of sequence $x(n)$, and \bar{y} represents the mean of sequence $y(n)$.

As described in the Section II, most traditional subcarrier fusion methods have one common characteristic which represents all subcarriers with one or several fused subcarriers for data dimension reduction [12] [22] [23]. However, only if two subcarriers are similar, one can be represented by the other. As shown in Fig. 5(a), the correlation between any two subcarrier sequences without co-channel interference is strong, the mean of its correlation coefficient can reach 0.85. Under such circumstances, it is reasonable to represent the features of other subcarriers with the fused subcarrier features.

However, Fig. 5(b) depicts the sequence correlation coefficient between any two subcarriers is rarely reach 0.3 in the scenario with co-channel interference, so it is unreasonable to use a fused subcarrier to represent other subcarriers. Two methods can be used to cope with the performance degradation of traditional subcarrier fusion methods caused by correlation weakened. In the first method, the strongly correlated subcarriers are selected to fuse. The second method is to select several weakly correlated subcarriers without fusing. The second method is more suitable than the first method for the scenario with co-channel interference. This is because the correlations between the spectrally-overlapped subcarriers and the non-overlapping subcarriers are weak. However, the correlations between subcarriers which in overlapping areas are strong, so do the subcarriers in non-overlapping areas. According to the first method, the strongly correlated subcarriers will be selected, so the fused subcarriers are either from the overlapping area or from the non-overlapping area, and the fused subcarriers from the first method do not contain the spatial characteristics of all subcarriers. Compared with the first method, the selected subcarriers from the second method contain more spatial characteristics of all subcarriers, this is because the subcarriers are selected from both overlapping area and non-overlapping area.

Based on the above analysis, a dynamic subcarrier selection method is employed in WiAnti with co-channel interference. The main idea of the subcarrier selection method is to select the weak correlated subcarriers without fusing. By using the features of selected subcarriers to represent all subcarrier characteristics, the data dimension and the loss of information can be reduced.

The subcarrier selection algorithm includes three steps:

- **Step 1** In each sliding window sample, subcarriers with weak correlation are selected, and the selected subcarriers form subcarrier combination.
- **Step 2** Through the statistical method, the subcarrier combination which has the most frequent occurrences is selected as input value of step 3.
- **Step 3** Because the same action reflects different phase changes for subcarriers whose center frequencies are different, the subcarriers in the selected subcarrier combination C_s should be selected from all three sections of [0, 10], [10, 20] and [20, 30]. If the output value of step 2 does not meet this condition, we choose the second most frequent subcarrier combination instead of the most frequent subcarrier combination, and the rest may be deduced by analogy.

In step 1, for each sliding window, we calculate inter-subcarrier correlation coefficients by Person's method to generate the correlation matrix $R_{x,y}$. The element $r_{x,y}$ in $R_{x,y}$ represents the coefficient of sequence correlation between subcarrier x and subcarrier y . We sort the elements which inside the matrix $R_{x,y}$ in ascending order to generate a new array I_f . According to the principle with the lowest correlation coefficient, we choose the two subcarriers with the weakest correlation. Subcarriers are gradually added to subcarrier combination according to the principle of the weakest total correlation until the number of subcarriers in subcarrier combination is n (the expected number of selected subcarriers). Finally, the selected subcarriers in each sliding window are determined.

In consideration of the interference changes in different sliding windows, we choose a subcarrier combination that fits all sliding windows. Step 2 is a effective statistic for the subcarrier combination in each sliding window. The mode of subcarrier combinations in all sliding windows is used as the input of step 3.

Because the phase of CSI is a important spatial feature and the same action has different phase changes on subcarriers of different center frequencies, the purpose of step 3 is to select the subcarrier combination which can represent the spatial characteristics of different subcarrier sections.

As for the complexity of the subcarrier selection algorithm, the complexity linearly increases with the data due to the fact that the method of Person's correlation coefficient used by the algorithm is linearly related to the data.

Algorithm 1 illustrates an algorithmic specification of the proposed dynamic subcarrier selection algorithm.

Algorithm 1 Dynamic Subcarrier Selection Algorithm

Input: CSI stream(i), the length of each stream is L .
Output: The selected subcarrier combination C_s , which contain n (Less than 30, the text is set to 5) subcarriers.

```

1: Initialize: The CSI stream is partitioned according to the
   sliding window size  $cw$ . Since there are  $i$  streams, the total
   amount of sliding windows is  $N = i \times \lfloor \frac{L}{cw} \rfloor$ .
2: for  $f <= N$ , where  $f$  represents the  $f^{th}$  sliding window
   do
3:   Calculate inter-subcarrier correlation coefficients ac-
      cording to Person's method to generate matrix  $R_{x,y}$ .
4:    $I_f :=$  the elements which inside the matrix  $R_{x,y}$  in
      accordance with the small to large order to generate an
      array  $I_f$ 
5:    $m_f := \min(I_f)$ 
6:   According to  $\text{corrcoef}(a, b) = m_f$ , select two subcar-
      riers with the weakest correlation ( $a$  and  $b$ ), at this point
       $C_f = \{a, b\}$ 
7:   while  $|C_f| <= n$  do
8:      $C_f =: C_f \cup new$ , make sure that the sum of the
      correlation coefficients between the  $new$  and the
      subcarriers in  $C_f$  is the smallest.
9:   end while
10:   $C := C \cup \{C_f\}$ 
11:   $f := f + 1$ 
12: end for
13: while  $C \neq \emptyset$  do
14:   if  $\text{Mode}(C) \cap [0, 10] \neq \emptyset$  and  $\text{Mode}(C) \cap [10, 20] \neq \emptyset$ 
      and  $\text{Mode}(C) \cap [20, 30] \neq \emptyset$  then
15:      $C_s := \text{Mode}(C)$ 
16:     break
17:   else
18:      $\forall C_{x \in [1, f]} = \text{Mode}(C), C - \{C_{x \in [1, f]}\}$ 
19:   end if
20: end while

```

D. Data Processing, Feature Extraction, and Classification

Data preprocessing has two main steps. Firstly, the weighted moving average is used to smooth CSI signal. Secondly, the sliding windows over data streams are used to segment the action samples, and the size of each sliding window is 500.

With the reference to the articles [10] [12] [23], totally, eight kinds of time domain features and two kinds of frequency domain features are selected. The time domain features are the mean of CSI, variance, maximum, minimum, median, first quartile, third quartile, and information entropy. The frequency domain features are spectrum energy and maximum frequency domain.

To evaluate the performance of dynamic subcarrier selection algorithm, four classical classification methods are used to recognize activities, which are the Random Forest (RF), the Decision Tree (DT), the Decision Tree Regression (DR) and the k-NearestNeighbor (kNN).

V. EXPERIMENT AND EVALUATION

This section illustrates the implementation and experimental evaluation of WiAnti. Firstly, the experimental settings are introduced. Then, the co-channel interference assessment is presented. Finally, the recognition accuracy rates of WiAnti and other systems in the scenario with co-channel interference are given.

A. Experimental Settings

As shown in Fig. 6, the experiment is conducted in the $6.1m \times 4m$ room which contains table and chairs for everyday use. The distance between point 1 and point 2 is 3 meters. The distance between laptop C and laptop D is 30cm. The router A and laptop C are placed in opposite positions. The model of two laptops is Thinkpad 420i, and the operating system is Ubuntu 14.04. Laptops C and D are equipped with Intel WiFi Link 5300 (i-wl5300) 802.11n NICs. The model of two routers is TL-WDR7500V3.0, which contains two 2.4GHZ band transmit antennas. All the NICs are equipped with three antennas, the 2×3 MIMO system produces six streams and achieves the spacial diversity.

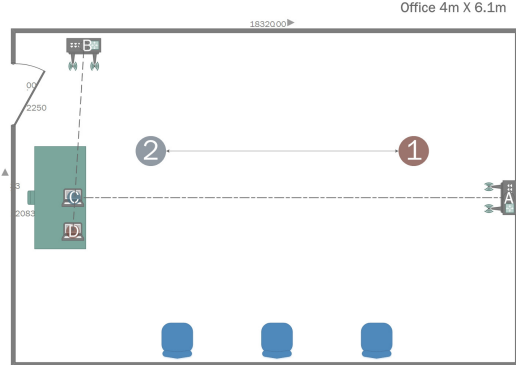


Fig. 6 The schematic diagram of experimental scene

Most of the activities such as lifting leg, closing leg and fall down happen in a few seconds. In order to capture the signal affect by these short time activities, the beacon rate should be set at 100 packets per second.

To measure the impact of interference on CSI, the following settings are necessary:

The scenario without co-channel interference and with co-channel interference comparison experiment is given.

In the scenario without co-channel interference, router A is set to channel 1, the laptop C and router A form a wireless link. At this point, the router B and laptop D are powered off.

In the scenario with co-channel interference, the router B is set to channel 3. The difference center frequency between the channel 3 and the channel 1 is 10 MHz, and the number of the spectrally-overlapped subcarriers occupy half of all subcarriers. Laptop D is connected to the router B, form a wireless link and the beacon rate of router B is set to 100 packets per second. The packet length is 25000 bytes, so the

amount of data generated by the router B per second is about 2.5 Mbytes.

We perform the experiment on six participants in both co-channel interference scenario and non-interference scenario. We also design four different actions, i.e., standing at point 1, walking between point 1 and point 2, running between point 1 and point 2 and sitting at point 1, and a reference state, i.e., empty room. Each participant provides 54 samples for each action and state. Actions are set to reflect the impact of co-channel interference on CSI with the movement of people, while empty room state reflects the impact of co-channel interference on CSI without human motion. Totally, $2 \times 6 \times 5 \times 54$ samples are collected for training and testing.

B. Co-channel Interference Assessment

By recording the number of CSI received packets per unit time, the existence of co-interference can be judged. The impact of subcarrier spectrally-overlap on packet reception is demonstrated by experiment. We change the channel of router B from 1 to 14. The rest of the settings are the same as Section V-A.

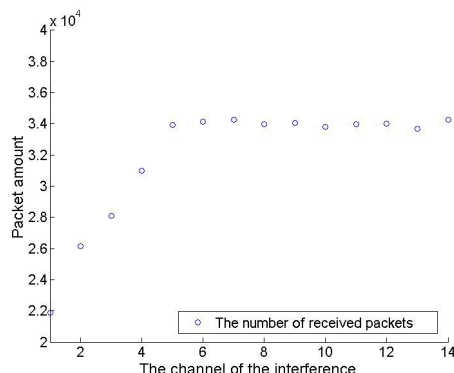


Fig. 7 The number of received packets in six minutes

Fig. 7 shows the number of packets received by laptop C in six minutes when the channel of B is different. Each experiment is repeated ten times, taking the average as the number of received packets per unit time. The experimental results can be divided into two cases. In the first case, we change the channel of router B from 6 to 14. In this case, the channel of router B and router A have no spectrally-overlapped subcarriers. The number of CSI received packets during six-minute is about 34000, smaller than the theoretical $6 \times 60 \times 100$, this is because WiFi is a wireless link, and instability is inherently due to attenuation or multipath effect. In the second case, the channel of router B is changed from 1 to 5, and router B and router A have spectrally-overlapped subcarriers. It can be seen from the Fig. 7 that the CSI received packets per unit time decrease. With the setting number of B's channel approaches to 1 (the channel of router A), the number of spectrally-overlapped subcarriers increases, leading to the probability of the channel enter back-off time increases, so the CSI received packets per unit time will decrease.

From the above analysis, by recording the number of CSI received packets per unit time and the CSI sampling frequency, the existence of interference can be determined.

C. Performance Evaluation

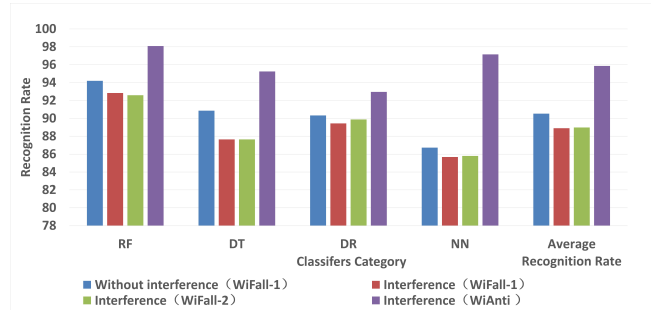
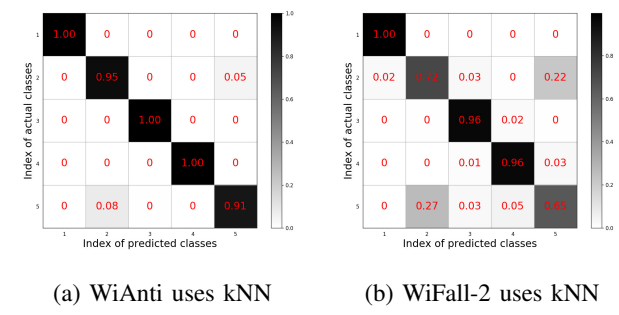


Fig. 8 Comparison Of Different Methods Of Recognition Accuracy Rates

A Python module *Scikit-learn* as the machine learning library is adopted to quickly realize RF, DT, DR, and kNN. In order to avoid overfitting, 10-fold cross-validation is used to train these classifiers. The recognition accuracy (RA) used in this paper is defined as the ratio of the number of correctly classified activities to the number of the whole testing activities, which can be expressed as follows,

$$RA = \frac{\text{number of correctly recognized activities}}{\text{number of whole testing activities}} \times 100\% \quad (6)$$

Fig. 8 shows the recognition accuracy rates of WiAnti compared with other methods in different classifiers. We find that WiAnti is capable of identifying activities accurately in the scenario with co-channel interference, by four different classifiers testing, WiAnti achieves 95.865% recognition accuracy rate on average, and the RF classifier can obtain the highest classification accuracy rate 98.09%. Compared to the baseline method WiFall-2, WiAnti gets 8% higher recognition accuracy rate in the scenario with co-channel interference.



(a) WiAnti uses kNN

(b) WiFall-2 uses kNN

Fig. 9 Confusion Matrix for Different Systems

In order to see the effects of co-channel interference on the performances of different systems, the two confusion matrices

are presented. The horizontal coordinates represent the type of predicted actions, while the vertical coordinates represent the actual type of actions, 1 to 5 represent a reference state, i.e., empty room, and four different activities, i.e., running, sitting, standing and walking. Fig. 9(a) shows the confusion matrix for WiAnti, compared with the confusion matrix for WiFall-2 as shown in Fig. 9(b), WiAnti can not only classify coarse-grained actions, i.e., empty rooms, sitting, standing, with high recognition accuracy rate close to 100%, but also achieve 95% of the fine-grained activities, i.e., walking and running recognition accuracy rate. Fig. 9(b) depicts WiFall can achieve pretty high classification rate in coarse-grained activities, however, co-channel interference has quite a big impact on the fine-grained activity recognition. In consideration of subcarrier correlation varies with co-interference, WiAnti gets less misclassification rate in fine-grained activities, 8% of the walking samples are judged as the running samples, while 5% of the running samples are judged as the walking samples.

VI. CONCLUSION

In this paper, we investigate the performance of CSI-based activity recognition system in the scenario with co-channel interference, and then we present WiAnti, a CSI-based activity recognition system which is robust to co-channel interference. WiAnti is based on a single commodity off-the-shelf WiFi device, which enables easy system set-up and maintenance. At the same time, a novel and dynamic subcarrier selection method is proposed. Compared with the traditional method, it can improve the recognition performance by 8% in the scenario with co-channel interference. For future work, we will discuss more effects of co-channel interference on CSI-based recognition system.

ACKNOWLEDGMENT

This work is supported by the National Natural Science Foundation of China (Grant No. 61202406). We would like to thank the anonymous reviewers for their comments.

REFERENCES

- [1] Oscar D Lara and Miguel A Labrador, "A survey on human activity recognition using wearable sensors," *IEEE Communications Surveys and Tutorials*, vol. 15, no. 3, pp. 1192–1209, 2013.
- [2] Marc Hassenzahl and Noam Tractinsky, "User experience-a research agenda," *Behaviour & information technology*, vol. 25, no. 2, pp. 91–97, 2006.
- [3] Wangjiang Zhu, Jie Hu, Gang Sun, Xudong Cao, and Yu Qiao, "A key volume mining deep framework for action recognition," in *Proceedings of the IEEE Conference on Computer Vision and Pattern Recognition*, 2016, pp. 1991–1999.
- [4] Lu Xia and JK Aggarwal, "Spatio-temporal depth cuboid similarity feature for activity recognition using depth camera," in *Computer Vision and Pattern Recognition (CVPR), 2013 IEEE Conference on*. IEEE, 2013, pp. 2834–2841.
- [5] Bingbing Ni, Gang Wang, and Pierre Moulin, "Rgbd-hudaact: A color-depth video database for human daily activity recognition," in *Consumer Depth Cameras for Computer Vision*, pp. 193–208. Springer, 2013.
- [6] Jess McIntosh, Charlie McNeill, Mike Fraser, Frederic Kerber, Markus Löchtefeld, and Antonio Krüger, "Empress: Practical hand gesture classification with wrist-mounted emg and pressure sensing," in *Proceedings of the 2016 CHI Conference on Human Factors in Computing Systems*. ACM, 2016, pp. 2332–2342.
- [7] Mathias Wilhelm, Daniel Krakowczyk, Frank Trollmann, and Sahin Albayrak, "ering: multiple finger gesture recognition with one ring using an electric field," in *Proceedings of the 2nd international Workshop on Sensor-based Activity Recognition and Interaction*. ACM, 2015, p. 7.
- [8] Qingchen Zhang, Laurence Tianruo Yang, Zhikui Chen, Peng Li, and Fanyu Bu, "An adaptive dropout deep computation model for industrial iot big data learning with crowdsourcing to cloud computing," *IEEE Transactions on Industrial Informatics*, 2018.
- [9] Qingchen Zhang, Laurence Tianruo Yang, Zheng Yan, Zhikui Chen, and Peng Li, "An efficient deep learning model to predict cloud workload for industry informatics," *IEEE Transactions on Industrial Informatics*, 2018.
- [10] Yan Wang, Jian Liu, Yingying Chen, Marco Gruteser, Jie Yang, and Hongbo Liu, "E-eyes: device-free location-oriented activity identification using fine-grained wifi signatures," in *Proceedings of the 20th annual international conference on Mobile computing and networking*. ACM, 2014, pp. 617–628.
- [11] Daniel Halperin, Wenjun Hu, Anmol Sheth, and David Wetherall, "Tool release: Gathering 802.11 n traces with channel state information," *ACM SIGCOMM Computer Communication Review*, vol. 41, no. 1, pp. 53–53, 2011.
- [12] Yuxi Wang, Kaishun Wu, and Lionel M Ni, "Wifall: Device-free fall detection by wireless networks," *IEEE Transactions on Mobile Computing*, vol. 16, no. 2, pp. 581–594, 2017.
- [13] Yu Gu, Fuji Ren, and Jie Li, "Paws: Passive human activity recognition based on wifi ambient signals," *IEEE Internet of Things Journal*, vol. 3, no. 5, pp. 796–805, 2016.
- [14] Heba Abdelnasser, Moustafa Youssef, and Khaled A Harras, "Wigest: A ubiquitous wifi-based gesture recognition system," in *Computer Communications (INFOCOM), 2015 IEEE Conference on*. IEEE, 2015, pp. 1472–1480.
- [15] Qifan Pu, Sidhant Gupta, Shyamnath Gollakota, and Shwetak Patel, "Whole-home gesture recognition using wireless signals," in *Proceedings of the 19th annual international conference on Mobile computing & networking*. ACM, 2013, pp. 27–38.
- [16] Karl Benkic, Marko Malajner, P Planinsic, and Z Cucej, "Using rssi value for distance estimation in wireless sensor networks based on zigbee," in *Systems, signals and image processing, 2008. IWSSIP 2008. 15th international conference on*. IEEE, 2008, pp. 303–306.
- [17] Wei Xi, Jizhong Zhao, Xiang-Yang Li, Kun Zhao, Shaojie Tang, Xue Liu, and Zhiping Jiang, "Electronic frog eye: Counting crowd using wifi," in *Infocom, 2014 proceedings ieee*. IEEE, 2014, pp. 361–369.
- [18] Linlin Guo, Lei Wang, Jialin Liu, and Wei Zhou, "A survey on motion detection using wifi signals," in *Mobile Ad-Hoc and Sensor Networks (MSN), 2016 12th International Conference on*. IEEE, 2016, pp. 202–206.
- [19] Stephan Sigg, Shuyu Shi, Felix Buesching, Yusheng Ji, and Lars Wolf, "Leveraging rf-channel fluctuation for activity recognition: Active and passive systems, continuous and rssi-based signal features," in *Proceedings of International Conference on Advances in Mobile Computing & Multimedia*. ACM, 2013, p. 43.
- [20] Fadel Adib, *See Through Walls with Wi-Fi*, Ph.D. thesis, Massachusetts Institute of Technology, 2013.
- [21] Bryce Kellogg, Vamsi Talla, and Shyamnath Gollakota, "Bringing gesture recognition to all devices," in *NSDI*, 2014, vol. 14, pp. 303–316.
- [22] Yunze Zeng, Parth H Pathak, and Prasant Mohapatra, "Analyzing shopper's behavior through wifi signals," in *Proceedings of the 2nd workshop on Workshop on Physical Analytics*. ACM, 2015, pp. 13–18.
- [23] Chunmei Han, Kaishun Wu, Yuxi Wang, and Lionel M Ni, "Wifall: Device-free fall detection by wireless networks," in *IEEE INFOCOM 2014-IEEE Conference on Computer Communications*, 2014.